

Insulin-like growth factor receptor I targeting in epithelial ovarian cancer

Walter H. Gotlieb^{a,b,*}, Ilan Bruchim^{a,b}, Jing Gu^{a,b}, Ying Shi^{a,b}, Anne Camirand^b,
Marie-José Blouin^b, Yunhua Zhao^b, Michael N. Pollak^{b,c}

^a Division of Gynecologic Oncology, McGill University, Montreal, Quebec, Canada

^b Lady Davis Institute of Medical Research, McGill University, Montreal, Quebec, Canada

^c Department of Oncology, McGill University, Montreal, Quebec, Canada

Abstract

Objectives. Preclinical evaluation of the anti-neoplastic activity of an insulin-like growth factor I receptor (IGF-IR) kinase inhibitor in ovarian cancer.

Methods. The OVCAR-3 and OVCAR-4 cell lines were investigated under serum-free tissue culture conditions. IGF-I and IGF-II production were evaluated by standard ELISA and immunohistochemistry. IGF-IR expression and protein levels were evaluated by Western blotting. Cytotoxicity assays were performed in triplicates using the Alamar colorimetric assay. Apoptosis was evaluated by flow cytometry and by Western blotting for PARP.

Results. The OVCAR-3 and OVCAR-4 cell lines produce IGF-I and IGF-II, and express IGF-IR, detectable by Western blotting, supporting the existence of an autocrine loop. The existence of this loop justified studies of NVP-AEW541, a small molecular weight inhibitor of the IGF-IR kinase. We observed growth inhibition of the ovarian cancer cell lines, with IC50 between 5 and 15 μ M. We also observed that NVP-AEW541 sensitized cells to cisplatin in vitro. Western blotting demonstrated that NVP-AEW541 induced apoptosis at the concentrations that were used in the cytotoxicity assays, and decreased the concentration of the phosphorylated AKT signaling protein downstream of the IGF-IR.

Conclusions. IGF-IR is a potential new molecular target in ovarian cancer. The anti-neoplastic activity of NVP-AEW541 in ovarian cancer was observed at concentrations higher than those previously reported for multiple myeloma, suggesting the possibility that a portion of the observed anti-neoplastic activity could involve targets other than the IGF-IR. Experiments are being conducted to investigate the cytotoxicity profile in vivo and the clinical relevance of NVP-AEW541 in ovarian cancer treatment.

Keywords: Insulin-like growth factor receptor; Kinase inhibition; Ovarian cancer; Cytotoxicity

Introduction

Epithelial ovarian cancer is the most frequent form of ovarian cancer, and develops from the malignant transformation of a single cell type, the ovarian surface epithelium, a single cell layer of peritoneum surrounding the ovary [1]. Most patients with epithelial ovarian cancer will have a satisfactory initial clinical response to aggressive cytoreductive surgery followed by combination chemotherapy, but unfortunately, this will usually not lead to cure [2]. The overwhelming majority of patients (>80%) will experience a recurrence. At present, no

surgery, chemotherapy, or radiation therapy regimen will salvage these patients. New treatment paradigms based on our growing understanding of molecular pathways associated with cancer growth are under investigation.

The insulin-like growth factor I receptor (IGF-IR) is a promising target because it is now recognized that this receptor is present on all ovarian cancer cells (reviewed in [3]), and its signaling leads to suppression of apoptosis, stimulation of proliferation, and constitutes an important cell survival pathway [4–6]. The IGF-I receptor is a heterodimeric transmembrane protein tyrosine kinase [7] with crucial role in organ development during embryogenesis, in regulating mitogenesis, and in cellular survival [8]. Phosphorylation of the IGF-I receptor occurs following binding of its ligand, the insulin-like growth factors I and II. This induces the recruitment of several effector mole-

* Corresponding author. Director Gynecologic Oncology, McGill University SMBD Jewish General Hospital, 3755 Cote Ste Catherine Road, Montreal Quebec, Canada H3T 1E2. Fax: +1 514 340 8619.

E-mail address: walter.gotlieb@mcgill.ca (W.H. Gotlieb).

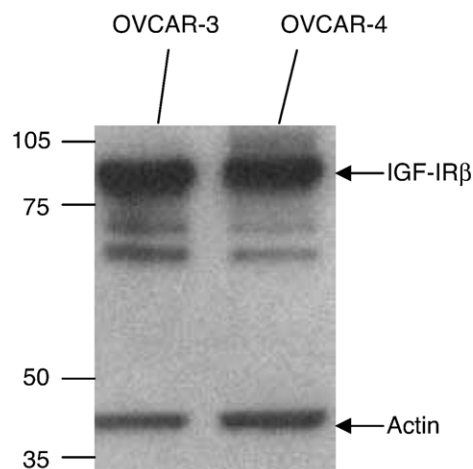


Fig. 1. Presence of IGF-I receptor protein in the OVCAR-3 and OVCAR-4 cell lines. Protein extracted from the OVCAR-3 and -4 cell lines, subjected to Western blotting, as detailed in Materials and methods, revealed high levels of protein for the 97-kDa IGF-I receptor β .

cules, in turn activating multiple signaling cascades. These cascades lead to proliferation and maintenance of cellular transformation.

In this manuscript, we evaluated the potential of NVP-AEW541, a pyrrolo[2,3-*d*] pyrimidine derivative that is capable of inhibiting the phosphorylation and activation of the downstream pathway components of the IGF-IR [9,10], to inhibit ovarian cancer cell proliferation, and to become a drug candidate to be evaluated in pre-clinical animal studies.

Materials and methods

Cell lines and treatment

The ovarian cancer cell line OVCAR-3 (American Tissue Culture Collection, Manassas, VA) and OVCAR-4 were grown in RPMI-1640 supplemented with 10% fetal bovine serum (FBS), 2 mM L-glutamine, and 10 μ g/ml of garamycin. The cells were routinely passaged every 5 to 7 days. Assays were performed in serum-free conditions.

NVP-AEW541, an IGF-IR kinase inhibitor, was obtained from Novartis Pharma AG (Basel, Switzerland) [9,10] and kept as a stock solution of 10 mM in DMSO.

Western blotting

Cells were lysed in radioimmunoprecipitation assay buffer (RIPA)(9.1 mM dibasic sodium phosphate, 1.7 mM monobasic sodium phosphate, 150 mM NaCl, 1% NP40, 0.5% sodium deoxycholate, 0.1% SDS, 0.2 mM sodium vanadate, 0.2 mM phenylmethylsulfonyl fluoride, and aprotinin at 0.2 units/ml). Clarified protein lysates (50 μ g) were resolved electrophoretically on denaturing SDS-polyacrylamide gels (8–10%), and transferred to nitrocellulose membranes. Membranes were probed with the following primary antibodies specific for: IGF-IR (Santa Cruz Biotechnology, Santa Cruz, CA), cleaved PARP (Biosource, Camarillo, CA), phospho-⁴⁷³Ser-AKT (New England BioLabs, Beverly, MA) and total AKT (New England BioLabs). Proteins were visualized with Horseradish peroxidase (HRP)-conjugated secondary antibodies (Amersham Biosciences, Baie-d'Urfé, QC). To confirm equal loading, membranes were stripped and reprobated using an antibody specific for Actin (Santa Cruz biotechnology). Antigen-antibody complexes were detected using the ECL system (Amersham Biosciences, Baie-d'Urfé, QC).

Cytotoxicity assays

For the cytotoxicity assays, monolayers of 2000 cells were plated into 96-well flat-bottom cell culture plates (Corning Incorporated, NY, USA) in medium containing 10% FBS. Twenty-four hours after plating, when the cells had attached and reached ~40% confluency, cells were washed and the medium was replaced with serum-free RPMI-1640 supplemented with 2 mM L-glutamine, and 10 μ g/ml of Garamycin. All experiments were performed for 96 h in serum-free conditions. Controls included 0.2% DMSO. NVP-AEW541 was used at concentrations ranging from 1.0 to 15.0 μ M. Cisplatin was obtained from Mayne Pharmaceuticals (Montreal, Quebec) and is provided by the company as a stock solution of 1 mg/ml. Cells were incubated for 4 h at 37°C with cisplatin ranging from 1 to 25 μ g/ml, then the medium was changed where indicated and the cells were further exposed to DMSO as control or to NVP-AEW541 at the concentrations indicated above. For the time course, cells were incubated under similar conditions for variable times ranging from 24 h to 72 h. All experiments were performed in triplicates and were reproduced and confirmed in at least three independent experiments. Cell viability was assessed by visual inspection of the plates and by using the AlamarBlue assay colorimetric assay. AlamarBlue (Biosource, Camarillo, CA) assay allows quantitative analysis of cell viability via the innate metabolic activity that results in a chemical reduction of AlamarBlue that changes from the oxidized (blue) form to the reduced (pink) form.

After cells were treated, AlamarBlue was added into the plates. When the color of the dye changed from blue to pink (around 6–18 h), plates were read in an ELISA plate reader at 2 different wavelengths, 562 nm and 620 nm to plot the graph. Percentage of reduced AlamarBlue was calculated using the following equation:

$$\text{Reduced AlamarBlue}(\%) = A_{562} - (A_{620} \times R_0);$$

where A_{562} and A_{620} are sample absorbencies minus the media blank; $R_0 = AO_{562}/AO_{620}$, AO_{562} = absorbance of oxidized form at 562 nm, AO_{620} = absorbance of oxidized form at 620 nm.

Immunocytochemical staining for IGF-II expression

The OVCAR-3 cells were plated on the Lab-Tek Chamber slide system (Nalgene Nunc, Naperville, IL), allowed to adhere for 48 h, and grown in serum-free medium. Cells were washed in PBS and fixed in 95% alcohol. Endogenous peroxidase was blocked with 30% hydrogen peroxide in methanol and then incubated for 15 min. Slides were submitted to protein blocking agent (Zymed) for 20 min in a humid chamber at room temperature. The slides were then incubated with diluted (1:50) anti-IGF-II mouse monoclonal IgG1 antibody clone S1F2 (Upstate laboratories, NY, USA) for 60 min at room temperature. Slides were washed in Tris buffer twice for 5 min each, and then incubated with biotinylated anti-mouse Ig for 30 min at room temperature in a humid chamber, and washed twice for 5 min with Tris buffer twice. Slides were incubated with SA-HRP for 30 min at room temperature in a humid chamber and rinsed in Tris buffer. This was

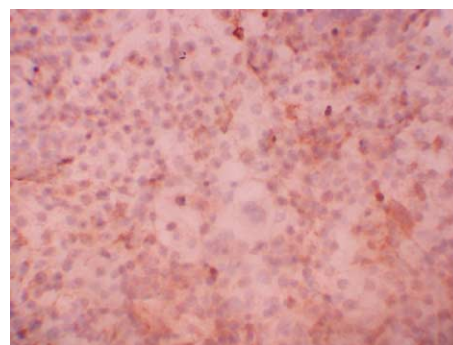


Fig. 2. Immunostaining for IGF-II. Following growth in serum-free medium, OVCAR-3 cells were incubated with anti-IGF-II mouse monoclonal antibodies identifying IGF-II production.

followed by incubation with DAB (1 drop of DAB and 1 drop of DAB H₂O₂) for 5 min, and rinsed in cold water. Slides were counterstained with hematoxylin for 10 s and washed with tap water for 5 min and dehydrated, cleared, and mounted.

ELISA for IGF-I and -II levels in supernatants from the cell line OVCAR-3

Monolayers of 1.2×10^5 cells were plated in 6-well flat-bottom cell culture plates. After 24 h, the cells were 60% confluent, and the medium was removed, plates were washed, and medium without FBS or phenol red was added. The media were collected after 24 h and 48 h respectively, and concentrated 30 times followed by analysis on an active IGF-I (DSL 10-5600) or IGF-II (DSL-10-9100) ELISA kit from Diagnostic Systems Laboratories, Inc. (Webster, TX). This is an enzymatically amplified “two-step” sandwich-type immunoassay. In the assay, standards, controls and unknown samples are incubated in microtitration wells, which have been coated with anti-IGF-I or -II antibody. After incubation and washing, the wells are treated with another anti-IGF-I or IGF-II detection antibody labeled with the enzyme horseradish peroxidase. After a second incubation and washing step, the wells are incubated with the substrate tetramethylbenzidine. We determined the degree of enzymatic turnover of the substrate by dual-wavelength absorbance measurement at 450 nm and 620 nm. The absorbance measured is directly proportional to the concentration of IGF present and compared to a set of IGF standards, used to plot a standard curve of absorbance versus IGF concentration.

Flow cytometry to assay apoptosis

OVCAR-3 cells (5×10^5) were plated in 60 mm dishes, to which either 0.2% of DMSO as control or the test concentration (15.0 μ M) of NVP-AEW541 were added for 72 h, (24 h prior to cytotoxicity assays) based on daily observation of the cells and performing the assay before the cells vanished. Supernatant was gently removed in an attempt to avoid removing poorly adherent dying cells. The cells were detached with trypsin-EDTA, pelleted by centrifugation, and washed twice with ice-cold PBS. Cells were resuspended in 100 μ l of annexin V buffer (10 mM HEPES/NaOH, pH 7.4, 140 mM NaCl, 2.5 mM CaCl₂) containing 5 μ l annexin V FITC and 10 μ l (50 μ g/ml) of propidium iodide (PI) using the APO-TARGET kit (Biosource, Camarillo, CA). After 15 min at room temperature, 400 μ l of annexin V binding buffer were added into each tube. Cells ($\pm 20,000$) were

analyzed by flow cytometry on a FASCalibur (Becton-Dickinson, Mountain View, CA).

Results

Expression of IGF-IR, IGF-I, and IGF-II protein levels in the OVCAR-3 and OVCAR-4 cell lines

Protein extracted from the OVCAR-3 and -4 cell lines and subjected to Western blotting revealed high levels of 97 kDa IGF-I receptor beta (Fig. 1). In order to evaluate for the presence of a potential autocrine IGF loop, we investigated for the presence of IGF-I or IGF-II protein. Medium recovered from cells grown for 24 h in serum-free condition, revealed the presence of 93.58 ng/ml IGF-II protein by ELISA. Following 48 h under the same conditions, the level of IGF-II increased to 162 ng/ml. In addition, immunocytochemical staining of OVCAR-3 cells grown in serum-free conditions showed staining for IGF-II (Fig. 2). ELISA for IGF-I showed that the levels of IGF-I in OVCAR-3 increased from 49 ng/ml in serum-free conditions after 24 h to 78 ng/ml after 48 h, and from 34 ng/ml to 42 ng/ml for OVCAR-4. In a first attempt to evaluate the potential of an autocrine loop, we incubated the cells with IGF-I, but could not detect any impact on cellular proliferation (Fig. 3), suggesting that the production of IGF-I and IGF-II by the cancer cells could be saturating the IGF-I receptor.

NVP-AEW541 inhibits the proliferation of OVCAR-3 and OVCAR-4 cells in a dose- and time-dependent manner, and potentiates the effect of cisplatin

Following the identification of the potential IGF-IR autocrine loop in OVCAR-3 and OVCAR-4 cells, we evaluated whether NVP-AEW541, a small molecular inhib-

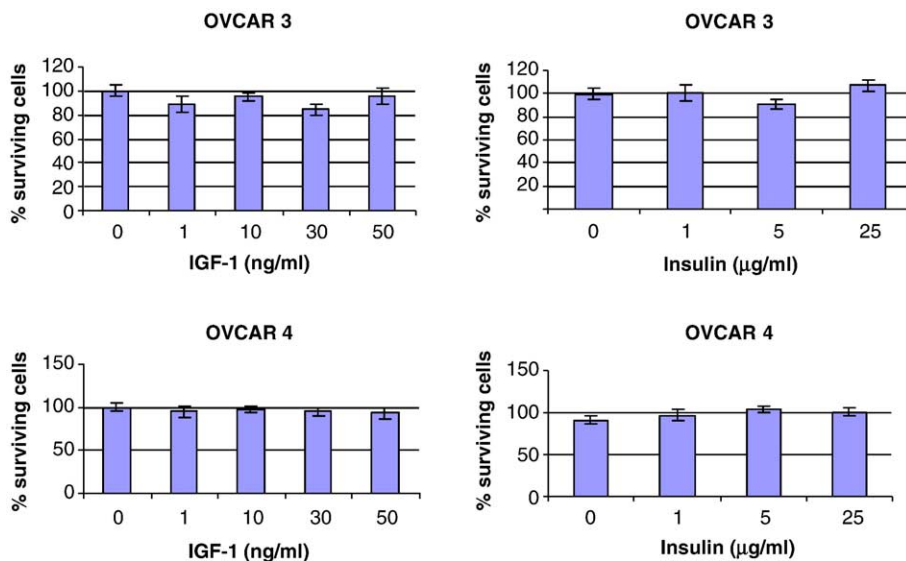


Fig. 3. Addition of IGF-I or Insulin does not impact on the cell growth of the OVCAR-3 or OVCAR-4 cell lines. Monolayers of cells, exposed to increasing doses of IGF-I or Insulin under serum-free conditions for 96 h, were assessed for viability using the AlamarBlue colorimetric assay. Results indicate that neither IGF-I nor Insulin influenced proliferation.

itor of the IGF-IR kinase, could inhibit cellular proliferation and further suggest the presence of an autocrine loop. OVCAR-3 and OVCAR-4 cells plated and exposed in serum-free conditions for 96 h to increasing doses (1 to 15 μM) of NVP-AEW541 showed a dose-dependent reduction in surviving cells with a LD50 between 5 and 15 μM (Fig. 4A). In addition to dose dependency, a time-dependent increase in toxicity was found (Fig. 4B). Add back of 50 ng/ml of IGF-I did not revert the NVP-AEW541 induced inhibition of proliferation (Fig. 4C). Results were corroborated with visual inspection of the plates and trypan blue exclusion (Fig. 4D).

Cisplatin is the most active treatment available for ovarian cancer. Similar to in vivo situations, the relative sensitivity of cells to cisplatin can vary somewhat, e.g., 2.5 $\mu\text{g/ml}$ cisplatin induces 75% toxicity in OVCAR-4 cells, while the same dose affects less OVCAR-3 cells, with a toxicity of 34% (Fig. 5A). This effect can be overcome by higher doses of cisplatin (e.g., 25 $\mu\text{g/ml}$ cisplatin, Fig. 5A).

In order to evaluate whether NVP-AEW541 could increase the toxicity of cisplatin on OVCAR-3 cells, co-incubation experiments using increasing doses of cisplatin with increasing doses of NVP-AEW541 were performed. At every dose of cisplatin, the addition of NVP-AEW541

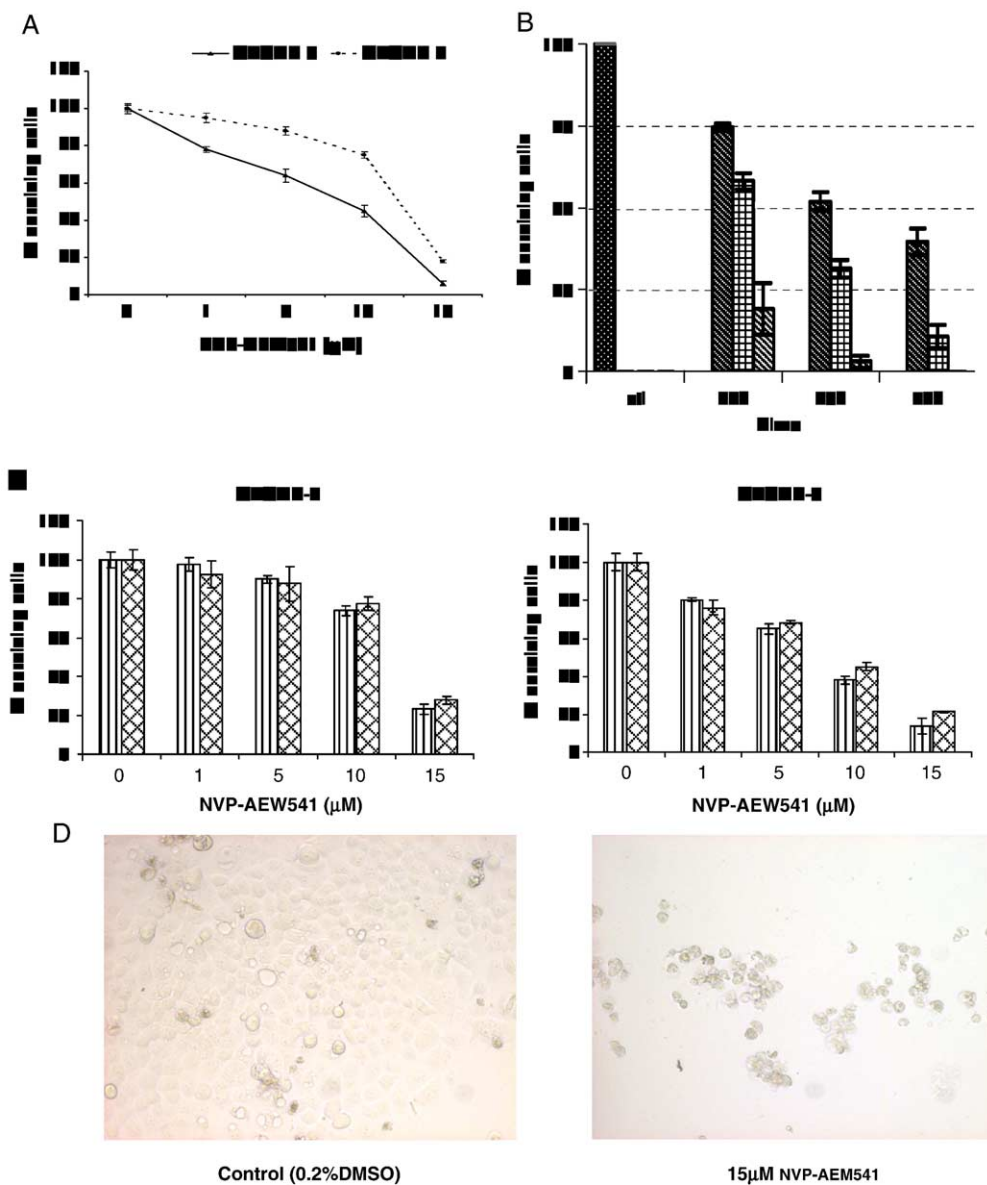


Fig. 4. NVP-AEW541 inhibits the proliferation of cells in a dose and time dependent manner that cannot be reversed by IGF-I. Monolayers of cells, exposed to increasing doses (A) of NVP-AEW541 for 96 h or for various periods (B), were assessed for viability using the AlamarBlue colorimetric assay. Results indicate a dose- (A) and time- (B) dependent toxicity. NVP-AEW541 ■, control; ▨, 10 μM ; ▩, 15 μM ; ▪, 30 μM . (C) Add back of 50 ng/ml of IGF-I does not revert the NVP-AEW541 induced inhibition of proliferation. Monolayers of cells were exposed to increasing doses of NVP-AEW541 in conjunction with 50 ng/ml of IGF-I. Viability was assessed using the AlamarBlue colorimetric assay. ▨, Medium; ▩, Medium supplemented with 50 ng/ml of IGF-I. (D) Photomicrograph of tissue culture dishes exposed to NVP-AEW541 as compared to control. Trypan blue exclusion following 96 h of culture in serum-free conditions under control conditions or 15 μM NVP-AEW541.

decreased the number of surviving cells in a dose dependent fashion (Fig. 5B).

Induction of apoptosis by NVP-AEW541

IGF-IR activation has been shown to protect cells from apoptosis. Interference with this mechanism by the IGF-IR kinase inhibitor, could explain the observed cell death observed in the cytotoxicity experiments. For these reasons, we investigated whether cells exposed to NVP-AEW541 underwent apoptosis. Cells exposed to 15 μM NVP-AEW541 for 48 h resulted in an increase in the proportion of apoptotic cells compared with control in both cell lines (Fig. 6). To further verify the apoptotic effect of NVP-AEW541, Western blot of PARP cleavage was used. As seen in Fig. 7A, treatment with 1 μM , 5 μM , 10 μM , and 15 μM NVP-AEW541 for 24 h gradually resulted in increasing amounts of cleaved PARP confirming the early signs of the induction of apoptosis. Fig. 5B shows the ratio of PARP protein over actin.

Decreased phosphorylation of AKT following IGF-IR KI

IGF-IR activation induces phosphorylation of AKT, which in turn has been implicated in the protection against apoptosis. In order to evaluate interference with downstream AKT activation by NVP-AEW541, Western blotting for phosphorylated AKT and AKT was performed (Fig. 8). Reduced levels of phosphorylated AKT with unchanged AKT levels were observed within minutes in the range of concentrations used to induce cytotoxicity.

Discussion

Recurrent ovarian cancer is generally treated with a variety of consecutive attempts at salvage chemotherapy regimens. These are associated with a concomitant increase in toxicity, together with a decrease in response from one regimen to the next, ultimately leading to death due to chemotherapy resistant tumor [11].

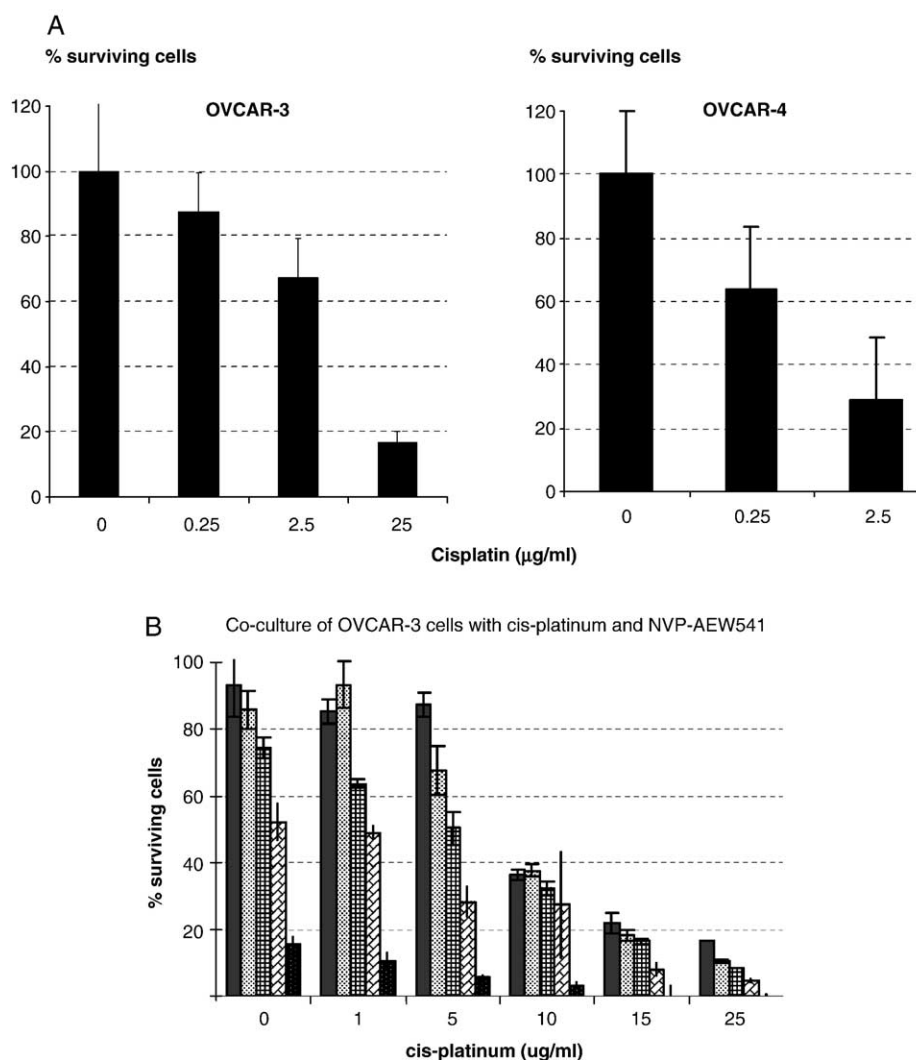


Fig. 5. Culture of OVCAR cells in the presence of increasing amounts of cisplatin with and without NVP-AEW541. (A) Cisplatin induces a dose dependent cytotoxicity. IC-50 for OVCAR-3 is between 2.5 and 25 $\mu\text{g/ml}$, whereas it is between 0.25 and 2.5 $\mu\text{g/ml}$ for OVCAR-4. (B) Addition of NVP-AEW541 potentiates the cytotoxicity induced by cisplatin. NVP-AEW541 \blacksquare , control; \square , 1 μM ; ▨ , 5 μM ; ▩ , 10 μM ; \blacksquare , 15 μM .

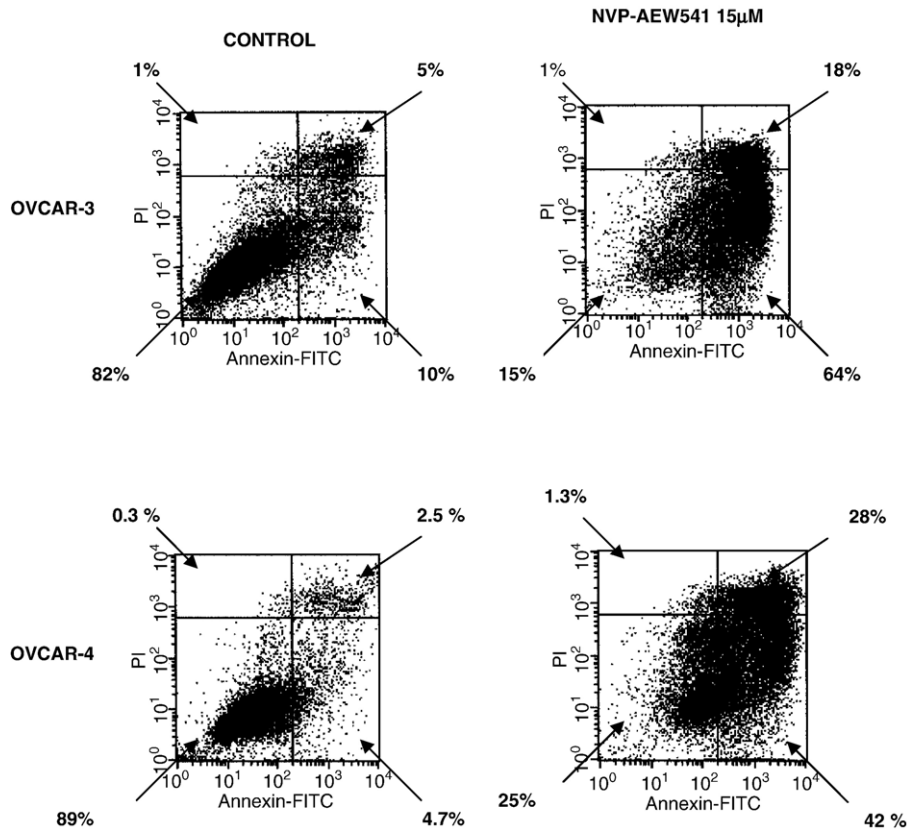


Fig. 6. Induction of apoptosis by NVP-AEW541. Flow cytometric analysis (PI versus Annexin-FITC) of OVCAR-3 and OVCAR-4 cells grown under control conditions (0.2% DMSO), or in the presence of 15 μ M NVP-AEW541.

There is a need to identify less toxic regimens that prolong survival of patients and to seek treatments that will transform response to treatment, into cure. Multiple pharmacokinetic approaches to overcoming drug resistance have

been attempted, but did not modify the overall survival of patients [12]. New paradigms are being sought to overcome the survival of chemotherapy resistant clones. In contrast to empirical treatments, targeted therapies rely on a growing

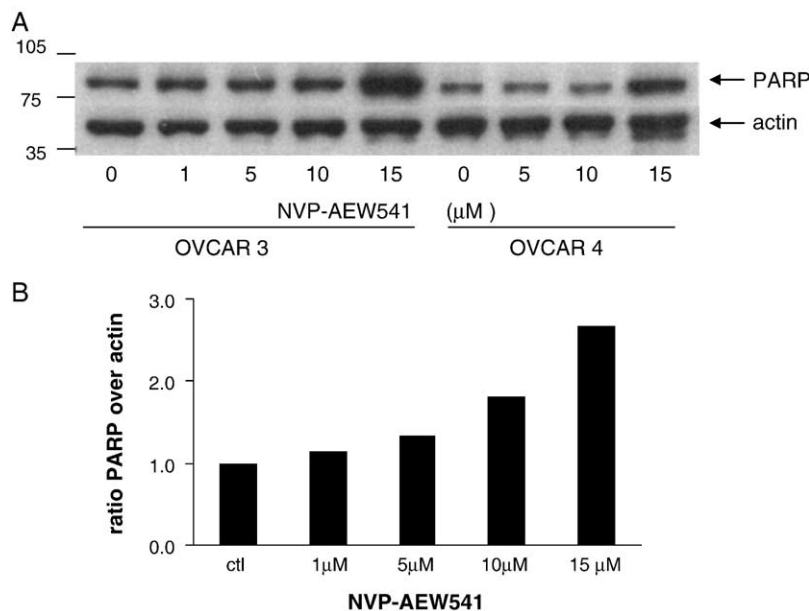


Fig. 7. Correlation between cleaved PARP and the induction of apoptosis by NVP-AEW541. (A) Protein extracted from OVCAR-3 and OVCAR-4 cells exposed to increasing doses of NVP-AEW541 was subjected to electrophoresis and Western blotting for PARP. (B) Ratio of band intensity for PARP over actin (for the OVCAR-3 cells) measured by densitometry.

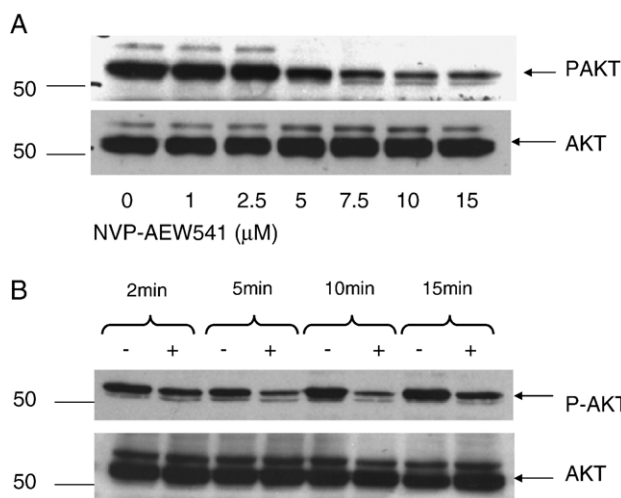


Fig. 8. Decreased phosphorylation of Akt following exposure to NVP-AEW541. Protein extracted from OVCAR-3 cells exposed to control conditions (0.2% DMSO), or (A) in the presence of increasing doses NVP-AEW541 (1 to 15 μ M for 10 min) or (B) for variable time periods: 2 to 15 min without (-) or with (+) NVP-AEW541 (15 μ M) were subjected to Western blotting for p-AKT and AKT.

knowledge of the molecular pathways in cancer cells [13,14].

Protein tyrosine kinases are now regarded as potentially important molecular targets.

The IGF-1 signaling pathway is involved in cellular proliferation and apoptosis, and interest in targeting this pathway has become widespread [15].

Insulin-like growth factors and their receptors are known to play key roles in regulating the normal biology of ovarian surface epithelial cells, and have been implicated in the transformed phenotype of ovarian carcinoma cells [3]. RNase protection assays originally revealed mRNA encoding IGF-I as well as IGF-IR in 100% of freshly isolated ovarian cancer specimens [16]. IGF-I levels were then found to be higher in cystic fluid from invasive malignant ovarian neoplasms as compared to cystic fluid from benign neoplasms [17]. Serum levels of IGF-I in patients with malignant ovarian tumors were significantly lower than in controls [18] but IGF-I serum levels have not been shown to be useful either in predicting the risk [19] or in the follow up of patients with ovarian cancer [20]. IGF-I, IGF-II, and the IGF-IR have also been shown to be produced *in vitro* by ovarian cancer cell lines [21], and various ovarian cancer cell lines display autocrine growth loops mediated through the IGF-I receptor [22]. We confirmed the presence of this potential autocrine loop in OVCAR-3 and OVCAR-4 cells. The cells produce IGF-I and II, and express the IGF-I receptor protein. Previously, antisense oligonucleotides to IGF-II were shown to significantly inhibit cell proliferation and induce apoptosis in human ovarian cancer cells [23]. In the context of the evidence for IGF-IR autocrine loop found in both the OVCAR-3 and OVCAR-4 cells, this manuscript presents evidence that interference with the IGF-IR kinase by NVP-AEW541 is associated with induction of apoptosis. Apart from its activity as a single agent, NVP-AEW541 also potentiates cisplatin. Co-incubation with cis-

platin demonstrated an increased cytotoxicity as compared to each agent used separately.

In many cell types, one of the key downstream pathways of the IGF-IR is AKT activation, which in turn stimulates cell survival [15]. We have shown that the inhibitory activity of NVP-AEW541 on both OVCAR-3 and OVCAR-4 is associated with the decreased phosphorylation of AKT, which is correlated with the observed decrease in proliferation and increase in apoptosis.

The concentrations of NVP-AEW541 found in this study to inhibit cell proliferation of the ovarian cancer cell lines are higher than the concentration found to be effective against multiple myeloma [10]. Multiple myeloma appeared to be the most sensitive to the effects of NVP-AEW-541 with IC50 values of 0.1–0.5 μ M. Higher IC50 values were observed in most other hematologic and solid tumor cell lines [10]. There are at least three possible explanations: (1) there may be differences in cellular and subcellular pharmacology of NVP-AEW541 between different cell types, and that effective intracellular concentrations are achieved at lower exposures in e.g. myeloma cells than ovarian cancer cells; (2) different cancers may have different degrees of IGF-IR dependence, and that, e.g., multiple myeloma cells are affected even when IGF-IR activity is partially inhibited, while other cancer cells are only affected at more complete levels of kinase blockade; and (3) in cancers where NVP-AEW541 is effective at higher concentrations than required for multiple myeloma cell inhibition, the compound may be acting on additional molecular targets that require somewhat higher concentrations, given the preferential inhibiting activity for the IGF-IR. Although we will need to investigate the precise mechanism of action further, from a pragmatic point of view, the clinical potential of NVP-AEW541 to inhibit ovarian cancer cell proliferation *in vivo* will depend on its therapeutic index rather than on its precise mechanism. Indeed, previous *in vivo* experiments using human tumor xenografts have raised the possibility of a favorable therapeutic index [10], but careful monitoring of toxicity (for example, related to glucose metabolism) will be required in animal experiments and in phase I evaluation of the compound. Lack of strict specificity for the IGF-IR kinase may contribute to the therapeutic benefit in ovarian cancer, provided that the occult kinases involved are contributing to the molecular pathology of the cancer, and that the compound is well tolerated at effective doses.

The clinical need for novel therapeutic approaches in ovarian epithelial cancer is widely acknowledged. In view of the evidence that an autocrine loop involving the IGF-IR contributes to the neoplastic behavior of ovarian cancer, further translational research regarding IGF-IR inhibition for this malignancy is justified.

Acknowledgments

This work was in part supported by grants from the Israel Cancer Research Foundation, the Montreal Center for Experimental Therapeutics in Cancer, the Fonds de recherche en santé du Québec, the Norych Career Scientist Award, the

Schouella Distinguished Scientist Award, and the Gloria Shapiro Foundation. NVP-AEW541 was graciously provided by Novartis Switzerland.

References

- [1] Jacobs IJ, Kohler M, Wiseman R, Marks J, Whitaker R, Kerns BJ, et al. Clonal origin of epithelial ovarian cancer: analysis of loss of heterozygosity, p53 mutation and x-chromosome inactivation. *J Natl Cancer Inst* 1992;84:1793–8.
- [2] Berek JS. Epithelial ovarian cancer. In: Berek JS, Hacker NF, editors. *Practical Gynecologic Oncology*. Philadelphia, PA: Williams and Wilkins; 2000. p. 457–522.
- [3] Kalli KR, Conover CA. The insulin-like growth factor/insulin system in epithelial ovarian cancer. *Front Biosci* 2003;8:d714–22.
- [4] Baserga R. The insulin-like growth factor I receptor: a key to tumor growth? *Cancer Res* 1995;55:249–52.
- [5] Wang Y, Sun Y. Insulin-like growth factor receptor-1 as an anti-cancer target: blocking transformation and inducing apoptosis. *Curr Cancer Drug Targets* 2002;2:191–207.
- [6] LeRoith D, Roberts Jr CT. The insulin-like growth factor system and cancer. *Cancer Lett* 2003;195:127–37.
- [7] Ullrich A, Gray A, Tam AW, Yang-Feng T, Tsubokawa M, Collins C, et al. Insulin-like growth factor I receptor primary structure: comparison with insulin receptor suggests structural determinants that define functional specificity. *EMBO J* 1986;5:2503–12.
- [8] Baserga R. The price of independence. *Exp Cell Res* 1997;236:1–3.
- [9] Garcia-Echeverria C, Pearson MA, Marti A, Meyer T, Mestan J, Zimmermann J, et al. In vivo antitumor activity of NVP-AEW541-A novel, potent, and selective inhibitor of the IGF-IR kinase. *Cancer Cell* 2004;5:231–9.
- [10] Mitsiades CS, Mitsiades NS, McMullan CJ, Poulaki V, Shringarpure R, Akiyama M, et al. Inhibition of the insulin-like growth factor receptor-1 tyrosine kinase activity as a therapeutic strategy for multiple myeloma, other hematologic malignancies, and solid tumors. *Cancer Cell* 2004;5:221–30.
- [11] Agarwal R, Kaye SB. Ovarian cancer: strategies for overcoming resistance to chemotherapy. *Nat Rev, Cancer* 2003;3:502–16.
- [12] Baird RD, Kaye SB. Drug resistance reversal—Are we getting closer? *Eur J Cancer* 2003;39:2450–61.
- [13] Muggia F, Lu MJ. Emerging treatments for ovarian cancer. *Expert Opin Emerg Drugs* 2003;8:203–16.
- [14] DiSaia PJ, Bloss JD. Treatment of ovarian cancer: new strategies. *Gynecol Oncol* 2003;90:S24–32.
- [15] Pollak M, Schernhammer ES, Hankinson SE. Insulin-like growth factors and neoplasia. *Nat Rev, Cancer* 2004;4:505–18.
- [16] Yee D, Morales FR, Hamilton TC, Von Hoff DD. Expression of insulin-like growth factor I, its binding proteins, and its receptor in ovarian cancer. *Cancer Res* 1991;51:5107–12.
- [17] Karasik A, Menczer J, Pariente C, Kanety H. Insulin-like growth factor-I (IGF-I) and IGF-binding protein-2 are increased in cyst fluids of epithelial ovarian cancer. *J Clin Endocrinol Metab* 1994;78:271–6.
- [18] Waksanski B, Dudkiewicz J, Kowalski T. Changes in insulin-like growth factor I, 17- β -estradiol, and progesterone in postmenopausal women with benign and malignant ovarian tumours. *Med Sci Monit* 2001;7:919–23.
- [19] Lukanova A, Lundin E, Toniolo P, Micheli A, Akhmedkhanov A, Rinaldi S, et al. Circulating levels of insulin-like growth factor-I and risk of ovarian cancer. *Int J Cancer* 2002;101:549–54.
- [20] Bese T, Nomir SK. The importance of serum insulin-like growth factor-I level determination in the follow-up of patients with epithelial ovarian cancer. *Eur J Gynaecol Oncol* 2001;22:372–6.
- [21] Conover CA, Hartmann LC, Bradley S, Stalboerger P, Klee GG, Kalli KR, et al. Biological characterization of human epithelial ovarian carcinoma cells in primary culture: the insulin-like growth factor system. *Exp Cell Res* 1998;238:439–49.
- [22] Resnicoff M, Ambrose D, Coppola D, Rubin R. Insulin-like growth factor-I and its receptor mediate the autocrine proliferation of human ovarian carcinoma cell lines. *Lab Invest* 1993;69:756–60.
- [23] Yin DL, Pu L, Pei G. Antisense oligonucleotide to insulin-like growth factor II induces apoptosis in human ovarian cancer AO cell line. *Cell Res* 1998;8:159–65.